

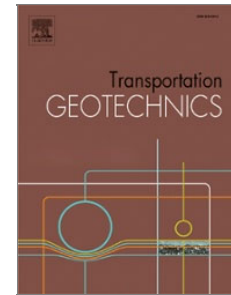
Please cite this article as:

Yepes J, García-González C, Franesqui MA (2020). *Rockfall hazard mitigation on infrastructures in volcanic slopes using computer-modelled ditches*. *Transportation Geotechnics* 25: 100402.  
DOI: <https://doi.org/10.1016/j.trgeo.2020.100402>

We are pleased to let you know that the final version of the article *Rockfall hazard mitigation on infrastructures in volcanic slopes using computer-modelled ditches* is now available online, containing full bibliographic details.

We have created a Share Link – a personalized URL – providing **50 days' free access** to this article.

Anyone clicking on this link before September 09, 2020 will be taken directly to the final version of this article on ScienceDirect, which they are welcome to read or download. No sign up, registration or fees are required:



<https://authors.elsevier.com/a/1bRln7tVeY57Gx>

# 1 **Rockfall hazard mitigation on infrastructures in volcanic slopes using computer-** 2 **modelled ditches**

3  
4 **Jorge Yepes**<sup>a</sup>, **Cándida García-González**<sup>b</sup>, **Miguel A. Franesqui**<sup>b\*</sup>

5 <sup>a</sup> Departamento de Ingeniería Civil – IOCAG, Universidad de Las Palmas de Gran Canaria (ULPGC),  
6 Campus de Tafira, 35017 Las Palmas de Gran Canaria, Spain.

7 <sup>b</sup> Grupo de Fabricación Integral y Avanzada – Departamento de Ingeniería Civil, Universidad de Las  
8 Palmas de Gran Canaria (ULPGC), Campus de Tafira, 35017 Las Palmas de Gran Canaria, Spain.

9 \* Corresponding author. E-mail address: [miguel.franesqui@ulpgc.es](mailto:miguel.franesqui@ulpgc.es) (Miguel A. Franesqui).  
10

## 11 **ABSTRACT**

12 Rockfalls on transport infrastructures are a serious hazard to users and many resources are invested in  
13 rock slope maintenance, stabilization, and protective measures. In volcanic territories, the risk of rock  
14 instabilities and rockfalls is very high due to the rugged natural slopes and origin of rock masses. With the  
15 aim of determining the influence of the geometric and material-related properties affecting rockfall  
16 motion and the effectiveness of catchment area design criteria, this study applies a computer simulation  
17 model considering 150 different slope configurations and ditch geometries, 4 types of materials and 9 size  
18 and shape combinations of falling rocks. A statistical analysis of the simulated rock stop-distances was  
19 performed. Results show that density, hardness, roundness and size are material properties directly  
20 correlated with the rockfall stop-distance. However, block accumulation distribution differs with the rock  
21 hardness. Furthermore, practical application design charts are proposed for infrastructure planning and  
22 design tasks. These offer the ditch dimensions depending on the relation between the optimal stop-  
23 distance and the cumulative percentage retained along the trajectory, complying with specific retention  
24 requirements, and optimize the dimensions of previous studies. A triangular ditch of foreslope steepness  
25 14° offered better retention capacity and road safety than a deep flat-bottom ditch. These rockfall  
26 protection areas constitute non-structural defence measures of reduced environmental impact and cost in  
27 volcanic territories.

28  
29 **Keywords:** Road slope; Rockfall catchment area; Ditch; Rockfall passive protection; Rockfall stop-  
30 distance; Volcanic terrain

## 31 **Highlights:**

- 32  
33 • Block density, hardness, stiffness, roundness and size show a direct correlation with the rockfall  
34 stop-distance.

- 35 • Triangular ditches with steeper foreslope gradient present higher retention capacity and better road  
36 safety than deep flat-bottom ditches.
- 37 • Block accumulation shows bimodal distribution for hard rock slopes, being unimodal for soft  
38 lithotypes.
- 39 • The ditch design charts proposed optimize the dimensions of rockfall catchment areas of previous  
40 studies.
- 41 • These defence ditches offer economic and environmental advantages compared to other structural  
42 solutions.

43  
44

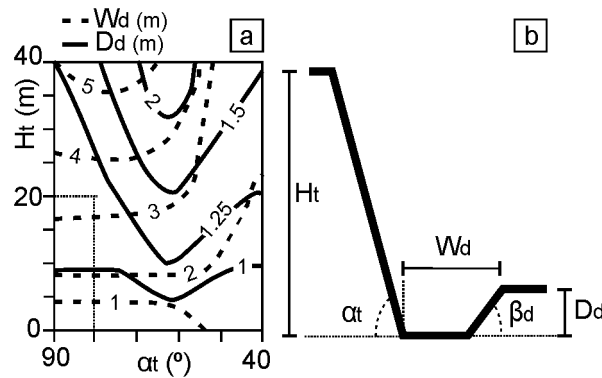
## 45 **1. Introduction**

46 In volcanic territories, such as many island regions with this geological origin, the risk of rock instability  
47 and rockfalls on transport infrastructures is prominent because of both topographical and lithological  
48 factors. The rugged natural relief makes it necessary to design roads and railways with limited width and  
49 steep adjacent slopes. The lithological characteristics, origin of rock masses, and even seismicity result in  
50 rock slopes with abundant potentially unstable blocks.

51 Rockfall protection does not have a single, clear solution. There is a wide range of possible situations that  
52 require specific treatment and engineering [1]. The use of catchment areas to reduce the hazardous  
53 consequences of rockfalls on transport infrastructures is a simple, economic and effective measure [2-5].  
54 It also means low environmental impact and easy maintenance. In fact, this is a competitive solution  
55 compared to stabilization structures (mesh, bolts, anchors) or defence constructions (dynamic rockfall  
56 barriers, retaining walls, fences, tunnels), that usually require important financial investment [4].  
57 Catchment areas are therefore an ideal method for protection of infrastructures in developing countries or  
58 with limited economic resources.

59 Ritchie (1963) [2] identified the characteristics of rockfall motion and proposed a graphic design chart  
60 and tables to determine the minimum depth and width of catchment ditches according to slope height and  
61 gradient, establishing the impact distance of a rockfall as a function of the slope height and steepness.  
62 This author proposed a deep flat-bottomed ditch (up to 2 m) of variable width, connected to the roadway  
63 by a constant foreslope ( $1.25H/1V$ ). This graphic chart and its version modified by the FHWA [6]  
64 represented a significant step forward in highway and railway protection design (Fig. 1). However,  
65 Ritchie's model is now seen to have some limitations: a) it does not provide a cost criterion allowing for  
66 choice of the most suitable capacity of block retention for each slope section; b) it offers results for only  
67 one geometry (trapezoidal ditch); and c) this deep and steeply-sloped ditch design makes it difficult for  
68 vehicles to return to the roadway safely as well as difficult maintenance of roadway margins.

69



70

71

**Fig. 1.** Rockfall catchment ditch design chart inspired upon Ritchie's work (1963): a)

72

Graphical chart to obtain ditch dimensions for a certain slope topographical configuration.

73

[E.g. for a slope 20 m high and at 80°, the proposed ditch has 3.3 m wide and 1.2 m deep];

74

b) Cross section of the slope-ditch configuration: ( $H_t$ ) Slope height, ( $\alpha_t$ ) Slope gradient,

75

( $W_d$ ) ditch width, ( $D_d$ ) Ditch depth, ( $\beta_d$ ) ditch gradient.

76

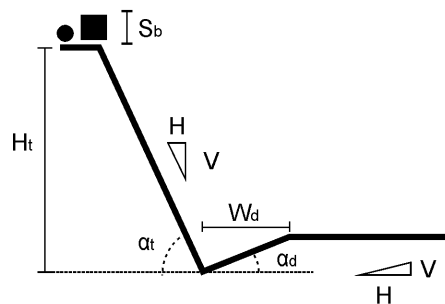
77 After Ritchie's research, some authors have evaluated the mechanics of rockfalls [7-16]. The Oregon  
 78 Department of Transportation (ODOT) carried out on site experimental work between 1992 and 1994,  
 79 gathering data from three types of catchment areas with different gradients (1H/0V or flat, 6H/1V and  
 80 4H/1V). To validate this work, blocks from different slope heights (40, 60 and 80 feet) over a constant  
 81 gradient (0.25H/1V) were rolled out [17]. The results provided an estimation of rockfall frequency,  
 82 quantified the probability of blocks reaching the road, and verified the retention capacity of catchment  
 83 areas. In 2001, the ODOT and the FHWA evaluated other configurations of the slope-ditch system. They  
 84 rolled 11,250 blocks of different sizes over different slope gradients (0.25H/1V; 0.5H/1V; 0.75H/1V and  
 85 1H/1V) and from differing heights (40, 60 and 80 feet). In this occasion, three kinds of triangular ditches  
 86 were evaluated (1H/0V; 6H/1V and 4H/1V). The results allowed new design charts to be drawn up [3].

87 A more economical and practical approach using numerous numerical simulation tools have been  
 88 developed based on the rockfall motion equations and interactions between the blocks and the slope [18-  
 89 23]. Pantelidis (2010) [4] used "RocFall" computer program (Rocscience, 2002) to develop adapted  
 90 graphic charts for catchment areas based on the Ritchie ditch: deep flat bottom, covered by a gravel layer  
 91 and with vegetation coverage at the edges. His research was based on the results of 100 rocks falling over  
 92 hard rock slope with a catchment area at the base. Moreover, Ref. [24] considered the use of additional  
 93 structures (fences and concrete walls).

94 Consequently, the catchment areas have not followed standardized design criteria. Those designed by  
 95 using empirical design charts may not be optimized and some might present unsafe conditions for road  
 96 traffic. Moreover, there are no standard specifications for computer-designed catchment areas at present.  
 97 As a result, there are many types of ditches —some oversized and others with low efficiency— which has  
 98 led to higher costs and higher environmental impact. Thus, new design criteria that are more rational and  
 99 quantitative must be found to solve this problem.

100 This study offers a useful tool to optimize the slope-bench-ditch system design, permitting easy  
 101 evaluation of its retention capacity at the planning stage or even when built, and justification of any  
 102 possible improvements. The criteria applied are quantitative and are based on numerical models. Five  
 103 different geometric factors were assessed to determine the stop-distance of rockfalls: shape ( $F_b$ ) and size  
 104 ( $S_b$ ) of the blocks, slope height ( $H_t$ ), slope gradient ( $\alpha_t$ ), and foreslope steepness of the catchment ditch  
 105 ( $\alpha_d$ ) [Fig. 2]. Both gradients (slope and ditch) are also expressed as a relation between the triangle sides  
 106 ( $H/V$ ). Moreover, other material-related factors such as density and hardness were also considered. This  
 107 produces a wide combination of possible values in these inputs, generating multiple arrangements and  
 108 output data.

109 The results obtained allow the estimation of the frequency of rock accumulation at different distances,  
 110 quantify the probability of these blocks reaching the roadway and verify the retention capacity of the  
 111 proposed catchment areas. These may be designed using the practical graphic charts produced in this  
 112 study. These rockfall protection ditches constitute defence measures with a reduced environmental impact  
 113 and much lower cost compared to other structural solutions. Furthermore, the interest and opportunity of  
 114 this topic acquires special relevance in order to save costs at the planning stage of construction projects  
 115 and also in the maintenance of transport infrastructures.



116  
 117 **Fig. 2.** Schematic cross section with the geometric parameters considered for modelling:  
 118 ( $S_b$ ) block size, ( $H_t$ ) slope height, ( $\alpha_t$ ) slope gradient, ( $W_d$ ) ditch width, ( $\alpha_d$ ) ditch  
 119 foreslope steepness. Different block shapes with diverse roundness coefficient are also  
 120 considered.

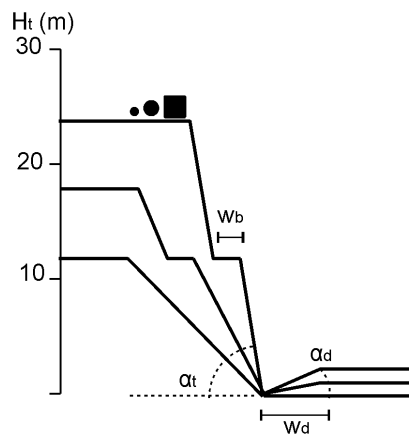
121  
 122 **2. Method**

123 When designing passive protection systems to mitigate rockfall hazards, standard practice is first to  
 124 simulate the block trajectory and then determine the optimal location and geometry for the chosen  
 125 solution according to the circumstances of the infrastructure to be protected. The “Colorado Rockfall  
 126 Simulation Program” (CRSP) was used to perform the simulation, as employed in previous studies  
 127 [20,25]. This computer program offers values for 4 rockfall parameters: velocity ( $V_i$ ), kinetic energy ( $E_k$ )  
 128 and block rebound height ( $H_r$ ), according to the established analysis partition, and the run-out distance  
 129 referred to the slope summit. These values allow to estimate the rockfall reach and evaluate the design of  
 130 block retention structures.

131 In our analysis 150 slope-bench-ditch topographic arrangements were considered, combining different  
132 slope heights ( $H_t$ ), slope gradients ( $\alpha_t$ ), and ditches of different foreslope steepness ( $\alpha_d$ ) (Fig. 3).  
133 Furthermore, two different extremal lithologies for the terrain (Hard Rock, HR; and Soft Rock, SR) were  
134 considered (see Table 2), so as any other lithology could have an intermediate performance. The  
135 geomechanical properties of the terrain (density [ $D_b$ ], hardness and stiffness [ $I_h$ ], roughness [ $R$ ]) and the  
136 block properties (shape or roundness [ $F_b$ ], size [ $S_b$ ]) were taken into account as determined following  
137 CRSP criteria [26]. The combination of all these variables defined 1,125 cases, each with 30 rockfall  
138 events analysed, giving a total of 33,750 results obtained.

139 Tables 1 and 2 summarize the different values of the parameters used for modelling: a) 5 slope heights  
140 ( $H_t$ ); b) 5 slope gradients ( $\alpha_t$ ); c) 2 slope configurations, including the presence of a bench (1 m wide) at  
141 12 m of the slope height; d) 3 ditch foreslope steepness ( $\alpha_d$ ); e) 4 materials (hard and soft rock for the  
142 natural slope, concrete for the ditch, and asphalt for the road pavement) with properties (density, stiffness  
143 and roughness) established according to references mentioned on Table 2; f) 9 combinations of possible  
144 blocks for hard rock and 6 for soft rock, depending on their shape (cubic, cylindrical, spherical) and size  
145 (0.3, 0.6 and 0.9 m; these correspond to frequent dimensions of rock blocks due to thermal retraction  
146 cracks generated during the cooling of volcanic geomaterials); g) the launch point of the blocks was  
147 random, along the entire slope, assuming that falling blocks start at rest. This is the most common  
148 situation on homogeneous and anisotropic slopes (a single rock type and the same weathering grade). The  
149 variation range of the parameters used for modelling covers the usual values in engineering projects  
150 constructed on rugged rock reliefs such as those in volcanic island territories.

151



152

153 **Fig. 3.** Modelled topographical cross sections with different configurations of the slope-  
154 bench-ditch-roadway system and the geometric factors considered for ditch design: block  
155 size, block shape, slope height ( $H_t$ ) [some including a bench ( $W_b$ )], slope gradient ( $\alpha_t$ ),  
156 ditch width ( $W_d$ ), and ditch foreslope steepness ( $\alpha_d$ ). The variation range of these  
157 parameters is detailed in Table 1.

158

159 **Table 1**

160 Geometric parameters of the slope-ditch system and blocks used in rockfall modelling.

Slope			Ditch		Block	
$H_t$ (m)	(H/V) <sub>t</sub> (m/m)	$\alpha_t$ (°)	(H/V) <sub>d</sub> (m/m)	$\alpha_d$ (°)	$F_b$ (-)	$S_b$ (m)
12	1/1	45	1/0	0	cube	0.3
15	1/2	63	6/1	9.4	cylinder	0.6
18 <sup>(*)</sup>	1/3	71	4/1	14	sphere	0.9
21 <sup>(*)</sup>	1/4	75				
24 <sup>(*)</sup>	1/6	80				

( $H_t$ ) Slope height; ( $\alpha_t$ ) Slope gradient; ( $\alpha_d$ ) Ditch foreslope steepness (both expressed as the relation between horizontal [H] and vertical [V] distances); ( $F_b$ ) Block shape; ( $S_b$ ) Block size; (\*) Slope with a 1 m wide bench located at a height of 12 m

161

162 Analysis required the following inputs: a) coordinates of the slope section; b) roughness and hardness of  
 163 the selected materials; c) launch location, number, shape and size of the blocks; d) specific weight of the  
 164 materials; e) analysis partition to obtain the results of the parameters analysed (velocity, kinetic energy,  
 165 block rebound height and roll-out stop-distance [ $X_{stop}$ ]). In this study, the analysis partition was located at  
 166 the edge of the roadway, so as to minimize the number of blocks reaching the road pavement.

167

168 **Table 2**

169 Geomechanical parameters of the different materials used in rockfall modelling.

Parameter	Value
Lithology (L)	Hard Rock (HR) Soft Rock (SR) Concrete (C) Asphalt (A)
Roughness (R); [m]	0.3-0.6 (HR) 0.3-0.6 (SR) 0.03-0.3 (C) 0.03-0.3 (A)
Hardness index ( $I_h$ ); [-]	0.8-1 (HR) 0.3-0.5 (SR) 1 (C) 0.9 (A)
Bulk density ( $D_b$ ); [kN/m <sup>3</sup> ]	23-24 (HR) 11 (SR) 24 (C) 23.5 (A)

(L) Lithology: HR (massive basalt) and SR (pumice) [27-29]; (R) Coefficient relating the slope surface geometry with the block radius [26]; ( $I_h$ ) Hardness index [related to the stiffness, to the tangential and normal restitution coefficients and to damping coefficients] [26]; ( $D_b$ ) Bulk density [27-29]

170

171 The software uses an algorithm with the general motion equations to simulate the block speed and the  
172 contact forces between the rock and the slope. Six parameters were used to simulate block impact: slope  
173 geometry, hardness and roughness of the terrain, density, shape and size of the block. Roughness is used  
174 to model the slope surface and is defined by a single value. Hardness is related to 2 coefficients [26]: the  
175 restitution coefficient (indicative of the impact elasticity) and the damping coefficient (indicative of the  
176 block tangential resistance). The computer simulation offers 5 outputs: velocity, kinetic energy, block  
177 rebound height and the roll-out stop-distance ( $X_{\text{stop}}$ ) referred to the analysis partition.

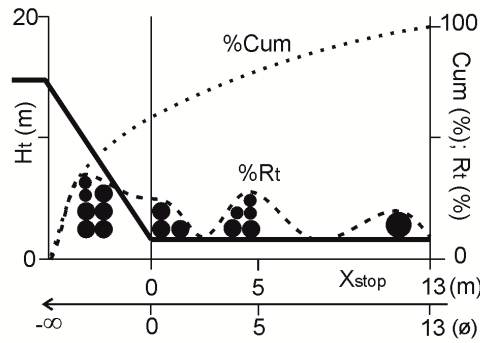
178 Results were classified depending on the lithotype, slope height, slope gradient, and type of catchment  
179 area. Each case was given an identification code according to its characteristics. In each case, the  
180 topographical configuration was represented by 2D slope cross sections, where the coordinate origin was  
181 located at the top of the slope. Stop distance ( $X_{\text{stop}}$ ) is shown on the X axis, and slope height ( $H_t$ ) on the Y  
182 axis. A 2-Dimensional approach is justified because this analysis focuses on constructed or excavated  
183 slopes, not on natural slopes and thus, these slopes are usually designed with the same gradient along  
184 certain distance, generating surfaces that can be assumed to be ideally plane.

185 In order to represent all the results in the same range of distances and to compare them, the origin of  
186 coordinates had to be displaced to the bottom of the slope. Therefore, the roll-out stop distances had to be  
187 modified by deducting the horizontal projection of the slope. These new distances were named as  
188 corrected distances. Based on these new values, statistical parameters were calculated to characterize and  
189 compare the 1,125 design cases (average, standard deviation, asymmetry, Kurtosis index).

190 At the same time, a change of variable was applied to the X-axis to represent the results as a Fi-normal  
191 distribution function and be able to establish statistic relations. The origin of the X-axis coincides with the  
192 base of the slope. Data distribution was restricted to the  $-\infty$  to +13 m range, so as to represent all the  
193 configurations. This range is able to include a maximum ditch width ( $W_d$ ) of 5 m, a roadway width of 8 m  
194 and any possible slope geometry ( $H_t$ ;  $\alpha_t$ ). These adjustments allowed to present the results of the 1,125  
195 cases analysed in the same range of normalized distances ( $X_{\text{stop}}^*$ ) and to establish comparisons between  
196 their basic aforementioned statistical parameters. All the roll-out stop distances data ( $X_{\text{stop}}^*$ ) are available  
197 in a supplementary file (see [Table 7](#) in [Electronic Supplementary Material](#)).

198 The range of distance values ( $-\infty$  to +13 m) was divided into unit sections (1 m). For each section, the  
199 absolute frequencies of retained blocks were calculated in percentages (%Rt) expressed in relation to the  
200 sum of all the events simulated for each case ( $n = 30$ ). The cumulative percentage (%Cum) was then  
201 calculated for each unit section ([Fig. 4](#)).

202



203

204

205

206

**Fig. 4.** Schematic representation of (%Rt) and (%Cum) distributions versus the stop-distance ( $X_{stop}$ ) based on Fi-normal distribution ( $\phi$ ). ( $H_t$ ) Slope height; (%Rt) Percentage of retained blocks; (%Cum) Cumulative percentage of block retention.

207

208

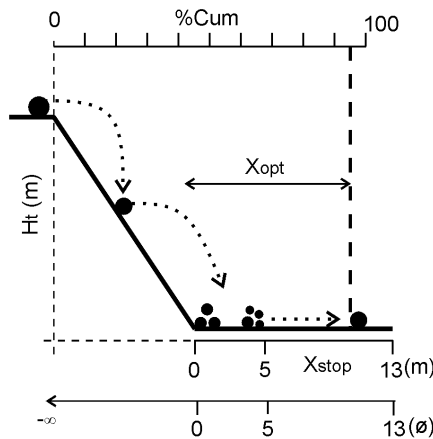
209

210

211

212

The optimal stop-distance ( $X_{opt}$ ) was determined based on the cumulative percentage (%Cum), and represents the distance corresponding to 95% of block retention. This estimation represents a reliability threshold of 95% in the ditch design, which is a frequent safety margin in civil engineering design.  $X_{opt}$  was calculated by interpolation of the closest values to 95%. Each geometric configuration and rockfall event has its own optimal stop-distance (Fig. 5).



213

214

215

216

**Fig. 5.** Graphical scheme of the cumulative percentage of retained blocks (%Cum) with regard to the block stop-distance ( $X_{stop}$ ). Example of a topographical cross section where the optimal stop distance ( $X_{opt}$ ) is calculated for a 95% of block retention.

217

218

219

220

A set of graphs were drawn up using all the optimal stop-distance values ( $X_{opt}$ ) in order to determine the influence of 5 factors on the block stop-distances. These factors were: slope height ( $H_t$ ), slope gradient ( $\alpha_t$ ), ditch steepness ( $\alpha_d$ ); shape ( $F_b$ ) and block size ( $S_b$ ). For each graph, the statistical distribution of values and fitting functions of 3 characteristic percentiles ( $P_{95}$ ,  $P_{50}$ , and  $P_5$ ) were analysed (Fig. 6).

221

222

223

224

Finally, graphical relations were determined between any cumulative percentage of rocks (%Cum) and the normalized stop-distance ( $X_{stop}^*$ ). For each slope configuration ( $H_t$ ,  $\alpha_t$ ), the (%Cum- $X_{stop}^*$ ) functions of the 3 types of ditches (flat [1H/0V], 10° [6H/1V] and 14° [4H/1V]) were plotted (see Fig. 13 in Electronic Supplementary Material). These ditch gradients are compatible with road traffic safety. The

225 design charts were only plotted for cubic blocks, because cubes are the most frequent block geometry in  
226 the lithotypes evaluated, both representative of volcanic hard rocks and soft rocks. These representative  
227 volcanic lithotypes were the massive basalt (HR) and the pumice (SR); this last type is a non-welded  
228 phonolitic ignimbrite. The geotechnical properties were obtained from Ref. [27-29]; these laboratory and  
229 field studies offer exhaustive data concerning most volcanic rock lithotypes.

230

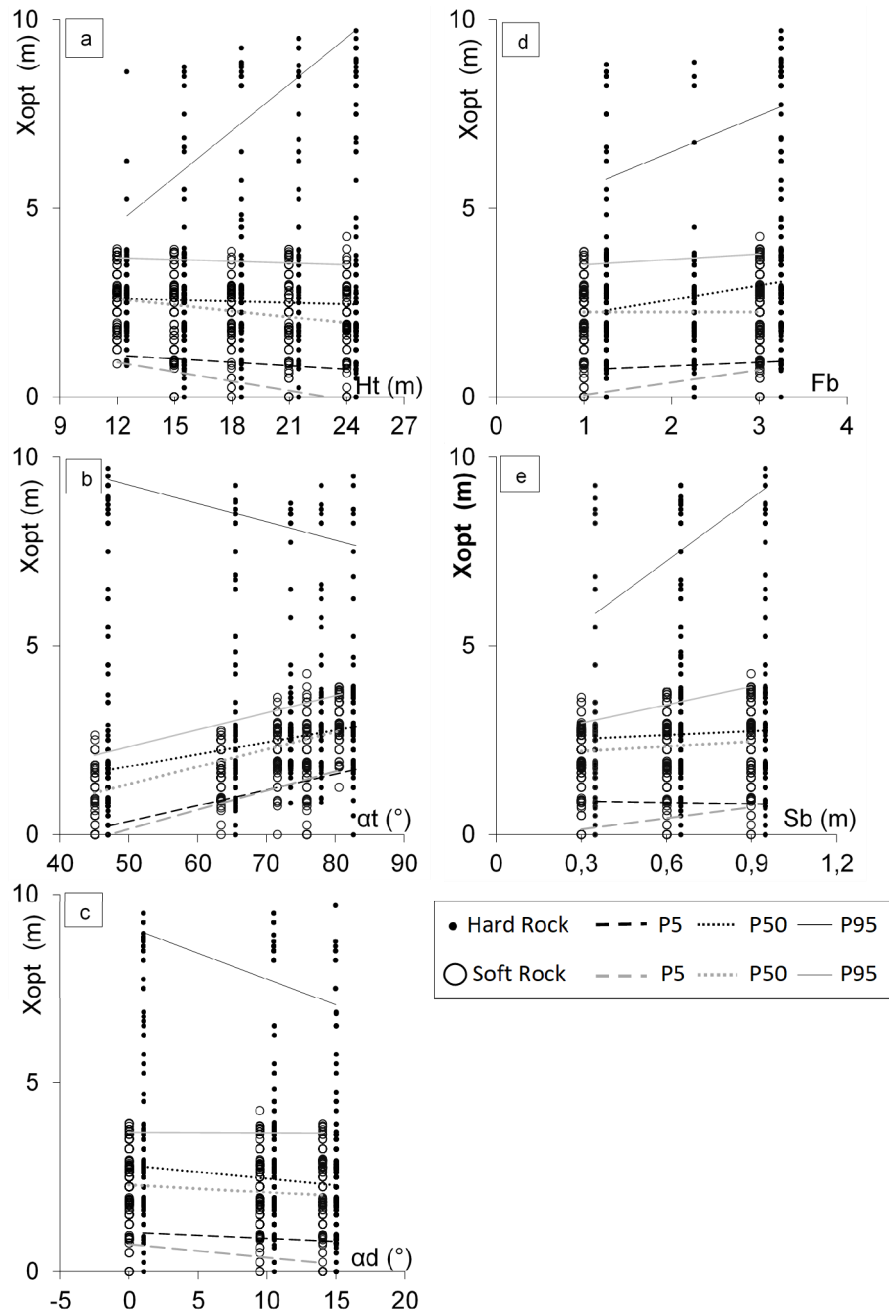
### 231 **3. Results**

232 The results generated have been distributed into three sections: a) Factors affecting the rockfall stop-  
233 distance, b) Practical charts to design and optimize the catchment areas, and c) Relations between the  
234 optimal ditch width and the topographical parameters.

#### 235 ***3.1. Influential factors of the rockfall stop-distance***

236 As detailed below, some observations were made after relating the optimal stop-distance ( $X_{opt}$ ) with the  
237 influential geometric factors:  $H_t$ ,  $\alpha_t$ ,  $\alpha_d$ ,  $F_b$  and  $S_b$  (Fig. 6). The linear fitting functions define a moderately  
238 good fitting, not only for hard rock (HR) but also for soft rock (SR). The parameters of the linear  
239 functions are shown in Table 3. However, the trend of the fitting function for percentile  $P_{95}$  in HR is  
240 usually very different compared to the rest of percentiles evaluated, especially in the representation of  $H_t$   
241 (Fig. 6a) and  $\alpha_t$  (Fig. 6b). It must be noted that statistical distributions of  $X_{opt}$  are always asymmetrical  
242 (positive skewness) with an average  $X_{opt} < 5$  m.

243



244

245

246

247

248

249

250

251

252

**Fig. 6.** Distribution of  $X_{opt}$  obtained by numerical simulation for the two lithotypes (Hard rock, HR; and Soft rock, SR). Each graph represents the relation between  $X_{opt}$  and a different geometric parameter: a)  $X_{opt}$  vs. slope height ( $H_t$ ); b)  $X_{opt}$  vs. slope gradient ( $\alpha_t$ ); c)  $X_{opt}$  vs. ditch steepness ( $\alpha_d$ ); d)  $X_{opt}$  vs. block shape ( $F_b$ ) [roundness code: (1) cube; (2) cylinder; (3) sphere]; e)  $X_{opt}$  vs. block size ( $S_b$ ). The fitting functions for the characteristic percentiles ( $P_{95}$ ,  $P_{50}$ ,  $P_5$ ) are also represented (see Table 3). Note: HR is represented by dots and SR by circles.

253  
254  
255

**Table 3**  
Linear fitting functions of  $X_{opt}$  characteristic percentiles ( $P_{95}$ ,  $P_{50}$ ) obtained after simulation.  
These functions are plotted in Fig. 6.

Functions		Hard rock (HR)		Soft rock (SR)	
		$P_{50}$	$P_{95}$	$P_{50}$	$P_{95}$
$X_{opt} = a \cdot H_t + b$	a	-0.0125	0.4103	-0.0533	-0.0154
	b	2.7563	-0.3292	3.2375	3.8707
	$\chi^2$	0.1023	0.8362	0.9018	0.1130
$X_{opt} = a \cdot \alpha_t + b$	a	0.0487	-0.0319	0.0461	0.0448
	b	0.2053	11.694	-0.9700	0.0821
	$\chi^2$	0.7245	0.9262	0.8197	0.7702
$X_{opt} = a \cdot \alpha_d + b$	a	-0.0343	-0.138	-0.0201	-0.0015
	b	2.8026	9.1271	2.2965	3.6846
	$\chi^2$	0.9592	0.6482	0.5583	0.0427
$X_{opt} = a \cdot F_b + b$	a	0.3750	0.9625	$2.0 \cdot 10^{-15}$	0.1429
	b	1.8229	4.5677	2.2500	3.3571
	$\chi^2$	0.5192	0.1134	1.0000	1.0000
$X_{opt} = a \cdot S_b + b$	a	0.3333	5.5417	0.4167	1.5961
	b	2.4333	3.9146	2.0833	2.4743
	$\chi^2$	0.5714	0.7500	0.7500	0.9424

( $H_t$ ) Slope height in m; ( $\alpha_t$ ) Slope gradient in degrees; ( $\alpha_d$ ) Ditch steepness in degrees; ( $F_b$ ) Block shape (cube = 1, cylinder = 2, sphere = 3); ( $S_b$ ) Block size in m; ( $\chi^2$ ) Chi-Square.

256  
257  
258  
259  
260  
261  
262  
263  
264  
265  
266  
267  
268  
269  
270  
271  
272  
273

$X_{opt}$  increases with increasing values of  $\alpha_t$ ,  $F_b$  and  $S_b$ . Thus, these factors have a direct relation with  $X_{opt}$  (Fig. 6b, Fig. 6d, Fig. 6e), although the function of percentile  $P_{95}$  in the representations of  $\alpha_t$  shows a negative trend for the HR lithotype (Fig. 6b). On the contrary, the observed trend of  $H_t$  and  $\alpha_d$  is negative. This means that these factors have an inverted relation with  $X_{opt}$  (Fig. 6a, Fig. 6c); however, it was found that the fitting function of percentile  $P_{95}$  for  $H_t$  shows a positive trend for the HR lithotype (Fig. 6a).

The  $X_{opt}$  distribution for SR is unimodal and is concentrated below the reference value ( $W_d$ )<sub>max.</sub> = 5 m accepted in this study. On the contrary, the dispersion of calculated values for  $X_{opt}$  in HR shows bimodal distribution. Blocks are concentrated near the base of the slope (1-4 m) and between 7 and 9 m. Both observations allow to define an optimal ditch width ( $W_d$ ) of 4 m for these materials.

These general trends present some nuances. On one hand, the  $X_{opt}$  distribution with regard to  $H_t$  has several gaps in HR slopes over 15 m high. These gaps can be observed when  $X_{opt} > 5$  m. Nevertheless, there is no clear linear relation concerning the space between gaps and slope height ( $H_t$ ) (Fig. 6a). On the other hand, it was found that ditch steepness ( $\alpha_d$ ) is more effective in steeper ditches ( $\geq 14^\circ$ ). Only in these cases, there is a significant reduction of rockfall stop-distance ( $P_{95}$ ) (Fig. 6c). Finally, there is also an important increase (1-2 m) in rockfall stop-distance for percentile  $P_{95}$  when the round shape of blocks increases (Fig. 6d).

### 274 3.2. Catchment area graphical design charts

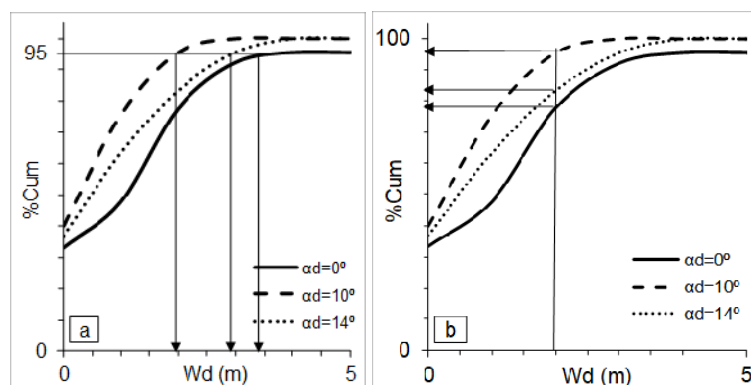
275 A total of 50 ditch design charts were drawn up, based on the relations between the cumulative  
 276 percentage of rocks (%Cum) and the rockfall stop-distance ( $X_{stop}^*$ ), one per slope configuration ( $H_t$ ,  $\alpha_t$ ).  
 277 All these graphics are included as [Electronic Supplementary Material](#) in Fig. 13. In each chart the  
 278 corresponding functions for ditches with different steepness (flat [1H/0V], 10° [6H/1V] and 14° [4H/1V])  
 279 are presented, including a horizontal line to represent the 95% percentile ( $P_{95}$ ) in order to facilitate  
 280 interpretation of the optimal ditch width ( $W_d$ ) capable of retaining the most suitable percentage of blocks  
 281 (%Cum) for designing tasks.

282 With these design charts it is possible to determine the suitable dimensions for ditches during the  
 283 planning stage following these 4 steps (Fig. 7a): 1) define the cross section geometry for the projected  
 284 slope ( $H_t$ ,  $\alpha_t$ ); 2) select the appropriate design chart (%Cum- $W_d$ ); 3) assume a certain reliability threshold  
 285 to obtain the desired percentage of retained blocks (%Cum). Most engineering projects frequently assume  
 286 a 95% of reliability (%Cum = 95%); 4) intersect the horizontal line with the curves for different ditch  
 287 steepness ( $\alpha_d$ ) and select on the X axis the most efficient ditch width ( $W_d$ ).

288 Likewise, these charts also make a possible inverse interpretation (Fig. 7b), and thus evaluate the  
 289 efficiency of an existing ditch ( $W_d$ ,  $\alpha_d$ ), for a specific slope configuration ( $H_t$ ,  $\alpha_t$ ), in 4 steps: 1) select the  
 290 appropriate design chart (%Cum- $W_d$ ) for the cross section geometry of the existing slope; 2) choose the  
 291 corresponding function with  $\alpha_d$  more similar to the steepness of the existing ditch; 3) intersect the vertical  
 292 line with the chosen curve and obtain on the Y axis the cumulative percentage of rocks (%Cum) that the  
 293 existing ditch would be able to retain; 4) evaluate whether the retained blocks percentage (%Cum) is  
 294 sufficient, or whether the assumed reliability percentage could be an unwanted risk factor.

295 In both analysis, the chosen option must be corroborated with a comparative cost assessment.

296



297

298 **Fig. 7.** Examples of graphic design chart interpretation. Here a case is considered with  
 299 the following parameters:  $H_t = 15$ ;  $\alpha_t = 75^\circ$ ;  $L = HR$ ;  $F_b = \text{cube}$ ;  $S_b = 0.9$  m: a) The %Cum  
 300 = 95% provides optimal ditch widths [ $2 \text{ m} < W_d < 3.5 \text{ m}$ ] able to retain 95% of potential  
 301 rockfalls; b) A ditch width  $W_d = 2$  m provides retention percentages between 78-95%,  
 302 depending on ditch steepness ( $\alpha_d$ ).

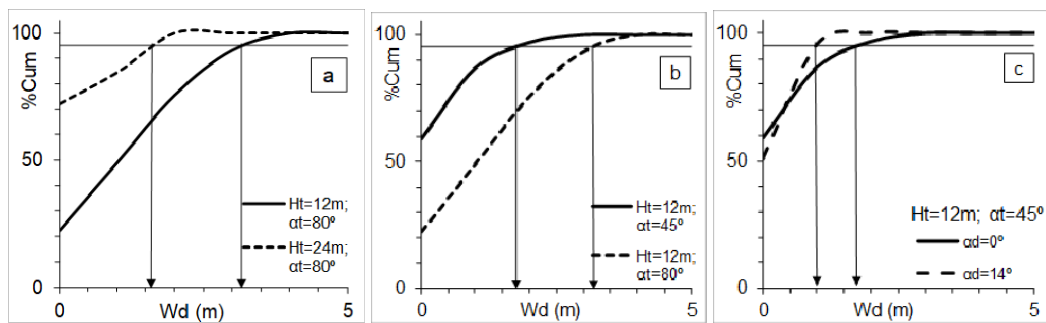
303

304 **3.3. Relations between the optimal ditch width and the topographical parameters**

305 The role of topography in the numerical modelling of stability of constructions in rock was assessed in  
 306 previous research [30]. The optimal catchment ditch width ( $W_d$ ) has certain relations with the geometric  
 307 factors ( $H_t$ ,  $\alpha_t$ ,  $\alpha_d$ ). Fig. 8 compares the  $W_d$  values for some different slope-ditch configurations varying  
 308 the aforementioned topographical parameters. In this figure the following observations can be drawn:

- 309 - An increase in slope height ( $H_t$ ) may obtain, under certain circumstances, the desired proportion  
 310 of block retention (%Cum = 95%) with lower values of  $W_d$ . Fig. 8a shows the comparison of two  
 311 extreme situations (different  $H_t$ ; the same  $\alpha_t$  and  $\alpha_d$ ) that confirms this observation.
- 312 - Secondly, an increase in slope gradient ( $\alpha_t$ ) may imply, under certain configuration of factors, an  
 313 increase in  $W_d$  to achieve a desired percentage of block retention. Fig. 8b compares two extreme  
 314 cases (the same  $H_t$  and  $\alpha_d$ ; different  $\alpha_t$ ) that bears out this observation.
- 315 - Thirdly, Fig. 8c shows that an increase in ditch steepness ( $\alpha_d$ ) reduces the  $W_d$  required to achieve  
 316 the expected percentage of block retention (%Cum = 95%).

317

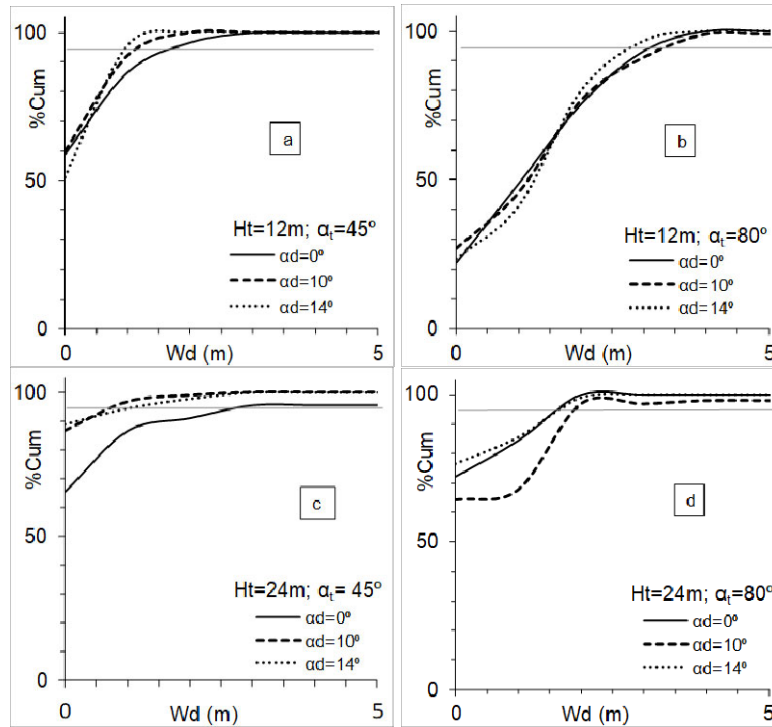


318

319 **Fig. 8.** Specific slope-ditch arrangements to show the influence of topographic and  
 320 geometric factors on the optimal  $W_d$ : a) Different slope height but same slope gradient  
 321 and ditch steepness; b) Same slope height but different slope gradient and ditch steepness;  
 322 c) Same slope height and slope gradient but different ditch steepness. ( $H_t$ ) Slope height;  
 323 ( $\alpha_t$ ) Slope gradient; ( $W_d$ ) Ditch width; ( $\alpha_d$ ) Ditch steepness; (%Cum) Cumulative  
 324 percentage of block retention.

325 Fig. 9 presents four representative situations from the 50 cases analysed. Each case shows the retention  
 326 capacity of the ditches with different steepness (flat [1H/0V], 10° [6H/1V] and 14° [4H/1V]) and width.  
 327 (The rest of design charts can be consulted in Fig. 13 as [Electronic Supplementary Material](#)).

328



329

330

331

332

333

334

335

336

#### 337 4. Final discussion

##### 338 4.1. Factors affecting the rockfall stop-distance

339 In this section the results obtained of rockfall stop-distance corresponding to 95% of block retention ( $X_{opt}$ )  
 340 leading to an optimal catchment ditch width ( $W_d$ ) are discussed in relation with the different factors  
 341 affecting them.

342 *Slope height ( $H_t$ ):*

343 A higher  $H_t$  means greater potential energy, thus suggesting in advance a longer stop-distance for 95% of  
 344 block retention ( $X_{opt}$ ). However, an increase of  $H_t$  also implies a longer trajectory and so energy loss due  
 345 to roll-out or rebound is higher. This fact can help to improve the retention capacity of the whole slope-  
 346 ditch system and explains certain results. Furthermore, the inverse correlation between the slope height  
 347 ( $H_t$ ) and the optimal catchment ditch width ( $W_d$ ) under certain configurations of the geometric factors (as  
 348 shown in Fig. 8a) could also be associated with the fact that the highest slopes analysed in this study ( $H_t \geq$   
 349 15 m) include a bench in mid-slope that may serve as an additional catchment area.

350 *Slope gradient ( $\alpha_i$ ):*

351 Rocks usually roll over moderate gradients (30°-45°) [2]. Friction between block and slope surface  
352 reduces the energy, slows the motion and, as a result, reduces the stop-distance ( $X_{opt}$ ). However, when  $\alpha_t$   
353 rises (45°-70°), the bounce probability increases and thus, friction decreases. This situation could be  
354 responsible of an increase in  $X_{opt}$  and of the direct correlation between the slope gradient ( $\alpha_t$ ) and  $W_d$   
355 observed in that cases (Fig. 8b). On the contrary, on steeper gradients (>70°-80°) blocks usually descend  
356 in free fall [8,31], impacting at the slope base and thus can reduce  $X_{opt}$ . Therefore, results suggest that  $X_{opt}$   
357 is greater for intermediate gradients, as established by other previous studies [32].

358 *Ditch steepness ( $\alpha_d$ ):*

359 An increase of  $\alpha_d$  improves the retention capacity of the whole catchment system (slope-ditch) because  
360 the rockfall stop-distance can be reduced due to the effect of foreslopes [3]. Thus, the inverse correlation  
361 between the ditch steepness ( $\alpha_d$ ) and  $W_d$  in all situations (Fig. 6c, Fig. 8c) would be related to the rebound  
362 direction change determined by such ditch foreslope, because blocks require more energy to keep rolling  
363 against the gravity. It can be observed that the influence of the ditch foreslope gradient ( $\alpha_d$ ) is effective in  
364 the steepest ditches ( $\geq 14^\circ$ ). Reduction of the optimal stop-distance ( $P_{95}$ ) is only significant in these cases.  
365 In flat ditches (1H/0V) the  $X_{opt}$  is almost 1,8 m larger than in steeper ditches (4H/1V) (Fig. 8c).

366 *Block shape and size ( $F_b$ ,  $S_b$ ):*

367 The less spherical the block, the larger the contact area between block and surface, meaning that the block  
368 has higher friction or resistance to movement [11,12,33]. In addition, more energy is needed to make  
369 blocks roll because they have to overcome more friction when rolling [9]. In contrast, the bigger the  
370 block, the higher the mass, so its initial potential energy partially counteracts the previously described  
371 effects, favouring an increase in  $X_{opt}$ .

372 *Bulk density ( $D_b$ ):*

373 The higher the density of the blocks, the more mass they have, and thus their superior initial energy  
374 results in greater distances. In addition, the hardness of the material generally increases and consequently,  
375 the kinetic energy loss is reduced at impacts. All these factors contribute to longer stop distances.  
376 Moreover, higher density normally means higher block resistance to fragmentation and this implies lower  
377 probability of breakage. Accordingly, the potential damage associated with rockfalls may be greater.

378 *Hardness index ( $I_h$ ):*

379 Hardness index ( $I_h$ ) depends on the restitution coefficient ( $K$ ) of the kinetic energy ( $E_k$ ) when an impact  
380 takes place ( $0 < K < 1$ ).  $K$  increases according to the material elasticity ( $\epsilon$ ). When  $\epsilon$  increases, the speed  
381 loss of the block is reduced ( $V_v = V_f - V_i$ ) at impacts and consequently the energy loss is also reduced. On  
382 the contrary, in slopes with low  $K$ , impacts are better absorbed and lose more  $E_k$ , meaning that stop  
383 distances ( $X_{opt}$ ) are shorter [7,34].

384 Table 4 summarizes, not in quantitative terms, the relations among every influential factor affecting block  
385 stop-distance and the performance variables involved in rock motion.

386

387 **Table 4**  
 388 Graphic summary of relations (direct or indirect) among the influential factors of rockfall stop-  
 389 distance and the different parameters related to rockfall performance (according to [Section](#)  
 390 [4.1](#)).

Material factors		Rockfall motion parameters					$X_{stop}$	
		M	E	$\epsilon$	$F_s$	$E_{loss}$	P <sub>50</sub>	P <sub>95</sub>
Bulk Density	(D <sub>b</sub> )	↑	↑	↑	↑	↓	↑	↑
Hardness Index	(I <sub>h</sub> )	-	-	↑	↓	↓	↑	↑
Roundness Coefficient	(F <sub>b</sub> )	-	-	-	↓	↓	↑	↑
Block Size	(S <sub>b</sub> )	↑	↑	-	-	-	↑	↑

Slope geometric factors		Rockfall motion parameters					$X_{stop}$	
		M	E	$\epsilon$	$F_s$	$E_a$	P <sub>50</sub>	P <sub>95</sub>
Slope Height	(H <sub>i</sub> )	-	↑	-	↑	↑	↓	↑
Slope Gradient	( $\alpha_i$ )	-	↑	-	↓	↓	↑	↓

Ditch geometric factors		Rockfall motion parameters					$X_{stop}$	
		M	E	$\epsilon$	$F_s$	$E_a$	P <sub>50</sub>	P <sub>95</sub>
Ditch Steepness	( $\alpha_d$ )	-	↓	-	-	-	↓	↓

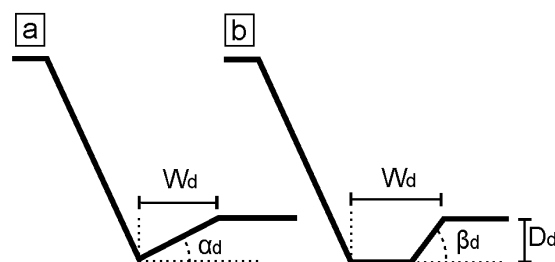
(M) Mass; (E) Total energy, equal to the sum of kinetic and potential energy; ( $\epsilon$ ) Elasticity; ( $F_s$ ) Friction strength; ( $E_{loss}$ ) Energy loss due to friction and elasticity; (P<sub>50</sub>) Percentile 50% of stop-distance statistical distribution; (P<sub>95</sub>) Percentile 95% of stop-distance statistical distribution. (Arrow pointing up means a direct relation between both parameters; if pointing down means an inverse relation).

391

#### 392 **4.2. Comparative analysis of catchment area designs**

393 Optimal catchment ditch widths ( $W_d$ ) according to several authors in different slope-ditch geometric  
 394 arrangements ([Fig. 10](#)) were compared. The results are summarized in [Table 5](#) and [Fig. 11](#). The  
 395 comparison of these results suggests that the performance of the steepest triangular ditch of constant  
 396 foreslope (used by Ref. [\[3\]](#) and this study) is more efficient (smaller  $W_d$  required) than the deep flat-  
 397 bottom ditch model (proposed by Ref. [\[2\]](#) and Ref. [\[4\]](#)).

398



399

400 **Fig. 10.** Examples of topographic cross section modelled with diverse slope-ditch  
 401 configurations: a) Ditch with foreslope steepness (Pierson et al., 2001; and this study); b)  
 402 Trapezoidal ditch (Ritchie, 1963; Pantelidis, 2010). The values of each parameter are  
 403 summarised in [Table 5](#): ( $W_d$ ) Ditch width; ( $\alpha_d$ ) Ditch steepness; ( $D_d$ ) Ditch depth; ( $\beta_d$ )  
 404 Ritchie's ditch foreslope gradient.

405

406 **Table 5**

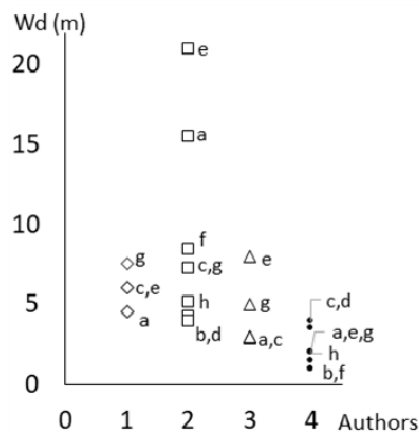
407 Comparative analysis of results for the optimal catchment area width ( $W_d$ ) in eight slope-ditch  
 408 geometric arrangements, according to different authors.

	$H_t$ (m)	12				24			
		$\alpha_t$ ( $^\circ$ )		$\alpha_d$ ( $^\circ$ )		$\alpha_t$ ( $^\circ$ )		$\alpha_d$ ( $^\circ$ )	
		45° (1H/1V)		80° (1H/6V)		45° (1H/1V)		80° (1H/6V)	
		0° (1H/0V)	14° (4H/1V)	0° (1H/0V)	14° (4H/1V)	0° (1H/0V)	14° (4H/1V)	0° (1H/0V)	14° (4H/1V)
	Ref.	(a)	(b)	(c)	(d)	(e)	(f)	(g)	(h)
<b>Ritchie (1963)</b>	$D_d$ (m)	1.5-1.8	-	1.2-1.5	-	1.8-2.1	-	1.5	-
	$\beta_d$	1/1.25	-	1/1.25	-	1/1.25	-	1/1.25	-
	$W_d$ (m)	4.6	-	4.6-6.1	-	4.6-6.1	-	6.1-7.6	-
<b>Pierson et al. (2001)</b>	$W_d$ (m)	15.5	4.3	7.3	4	21	8.5	7.3	5.2
<b>Pantelidis (2010)</b>	$D_d$ (m)	1	-	1	-	1	-	1	-
	$\beta_d$	1/1	-	1/1	-	1/1	-	1/1	-
	$W_d$ (m)	3	-	<3	-	8	-	3-5	-
<b>This study</b>	$W_d$ (m)	2	1	4	3.5	2	1	2	1.5

( $H_t$ ) Slope height; ( $\alpha_t$ ) Slope gradient; ( $\alpha_d$ ) Ditch steepness; ( $\beta_d$ ) Trapezoidal ditch foreslope; ( $D_d$ ) Trapezoidal ditch depth; ( $W_d$ ) Optimal ditch width; (Ref.) Reference of each geometric arrangement and  $W_d$  value represented in Fig. 11. Note: the slope gradient and ditch gradient are both expressed as the relation between horizontal [H] and vertical [V] distances (H/V)

409

410 It is worth noting that the optimal ditch width values ( $W_d$ ) obtained in our work are significantly lower  
 411 than the results from previous studies (Fig. 11). The percentage reduction of  $W_d$  in the present study in  
 412 comparison to designs of previous authors varies over a wide range (12% to 90%) depending on the  
 413 assumptions (Table 6). This could be related to the criterion assumed when modelling (random heights of  
 414 launch points).



415

416 **Fig. 11.** Graphical representation of the optimal ditch width ( $W_d$ ) values, according to  
 417 different authors, summarised in Table 5. Authors: (1) Ritchie [1963]; (2) Pierson et al.  
 418 [2001]; (3) Pantelidis [2010]; (4) This study.

419

420 **Table 6**  
 421 Summary of the percentage reduction of the optimal catchment ditch width ( $W_d$ ) of the present  
 422 study in comparison to the proposals of previous authors.

Author	Geometric arrangement (Ref. according to Table 5)							
	(a)	(b)	(c)	(d)	(e)	(f)	(g)	(h)
Ritchie (1963)	-56.5	-78.3	-34.4	-42.6	-67.2	-83.6	-73.7	-80.3
Pierson et al. (2001)	-87.1	-76.7	-45.2	-12.5	-90.5	-88.2	-72.6	-71.1
Pantelidis (2010)	-33.3	-66.6	+33.3	+16.7	-75.0	-87.5	-60.0	-70.0

Reduction of the optimal  $W_d$  (%) =  $(W_{d1} - W_{d2}) / (W_{d2}) \times 100$ ;

where:  $W_{d1}$ : optimal ditch width calculated in this study;  $W_{d2}$ : optimal ditch width calculated by previous authors.

Negative values indicate a percentage reduction, meaning that the optimal  $W_d$  proposed in this work is smaller.

423

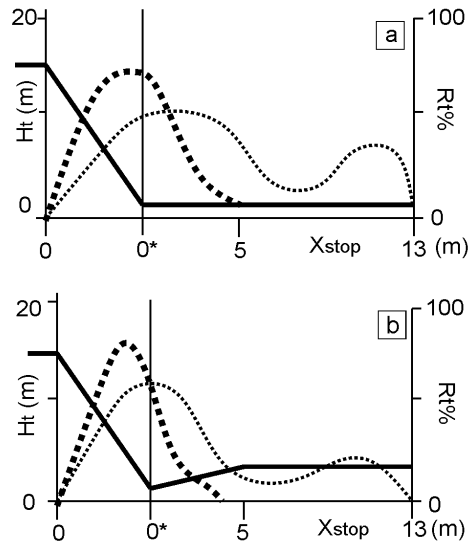
424 The present study analyses rockfalls on homogeneous but anisotropic slopes with only one rock type and  
 425 the same degree of alteration and weathering (RMR), because in volcanic materials the different main  
 426 layers are usually sub-horizontal and with a thickness of tens of metres. Moreover, these assumptions  
 427 allow to simplify modelling (summing up a total of 1,125 cases and 33,750 results). For rockfall  
 428 modelling we assumed that launch points were randomly distributed along the entire slope. Other authors  
 429 have preferred to consider exclusively launch positions located at the slope summit. However, the  
 430 hypothesis proposed here encompasses the most common situations, because the probability of finding  
 431 unstable blocks is similar along the entire slope under the assumptions aforementioned. Geotechnical  
 432 studies suggest that rockfall launch locations are not always at the top of the slope, because they can be  
 433 affected by several factors: e.g., the increase of horizontal stress against the slope wall towards the foot of  
 434 the slope; amplification of instability due to undermining of a soft layer under a hard layer; accelerated  
 435 weathering affecting the slope at points of aquifer discharge, etc. Thus, the hypothesis here proposed  
 436 would allow more realistic technical studies to be drawn up and thus provide more economic solutions  
 437 and more suitable to the service life of transport infrastructures.

#### 438 **4.3. Conceptual model of block accumulation in the catchment area**

439 The statistical analysis of the absolute frequencies of blocks retained at each distance in the slope-ditch  
 440 system establishes the block concentration areas depending on the ditch steepness and lithotype of rock.  
 441 Results of roll-out stop-distances for the 1,125 cases analysed are available in a supplementary file (Table  
 442 7 in Electronic Supplementary Material).

443 For hard rock (HR) slopes in both ditch configurations (flat or foresloped ditches), statistical distribution  
 444 of events shows a bimodal trend, with two areas of block concentration. Blocks tend to concentrate at the  
 445 base of the slope (0-4 m) and between 7 to 9 m if the ditch presents a foreslope gradient. These distances  
 446 increase nearly 2 m with a flat ditch (Fig. 12).

447 On the contrary, in the case of soft rock lithotype (SR) the stop-distance distribution is unimodal in both  
 448 ditch configurations and blocks are located at 95% below 4-5 m from the slope base (Fig. 12).



449

450

451

452

453

454

455

## 456 5. Conclusions

457

458

Based on the results and discussion of this research, the following conclusions can be drawn regarding rockfall catchment area modelling and the factors involved:

459

460

461

462

463

464

465

466

467

468

469

470

471

472

- The material-related factors used in the simulation process (density  $D_b$ ; hardness  $I_h$ ; block roundness  $F_b$ ; and block size  $S_b$ ) show a direct correlation with the rockfall computer-simulated stop-distance ( $X_{stop}$ ).
- The ditch steepness ( $\alpha_d$ ) presents an inverse relation with  $X_{stop}$ , meaning that steeper ditch foreslopes efficiently improve the retention capacity.
- However, the slope geometric factors (height  $H_t$ , gradient  $\alpha_t$ ) present uneven relations with  $X_{stop}$ . For hard rock lithotype (HR) and with the stop-distance retaining 95% of blocks ( $P_{95}$ ),  $H_t$  has a direct correlation and  $\alpha_t$  has inverse correlation, whereas with percentiles lower or equal than 50% the correlations are reversed. Numerical results suggest that the rockfall stop-distance is greater for intermediate slope gradients ( $45^\circ$ - $70^\circ$ ).
- For hard rock (HR) slopes, both with flat and with foresloped ditch, rock accumulation shows a bimodal statistical distribution, with two areas of block concentration. Blocks tend to concentrate at the base of the slope (0-4 m) and between 7 to 9 m if the ditch presents a foreslope gradient. These distances increases nearly 2 m with a flat ditch. By contrast, in case of soft rock lithotype

473 (SR) the stop-distance distribution is unimodal in both ditch configurations and blocks are  
474 located below 4-5 m from de slope base.

475 • Factors related to rock hardness and strength ( $D_b$ ,  $I_h$ ) produce an amplification of the rockfall  
476 stop-distance (longer  $X_{opt}$  and bimodal distribution) and an increase of hazard associated with  
477 rockfall on infrastructures due to lower energy loss for blocks and inferior probability to be  
478 broken or fragmented. The effectiveness of the catchment area is then more evident at higher  
479 values of the ditch steepness.

480 • The slope geometric conditions are decisive for rockfall stop-distances. Re-excavation of the  
481 slope top or wider benches at half slope height with a foreslope gradient could increase the  
482 retention capacity of the slope-bench-ditch system. On the contrary, a flat and excessively  
483 narrow bench at half slope height could act as a sky jump board and make stop distances longer.

484 • The catchment area graphical design charts drawn up allow the determination of the suitable  
485 dimensions for ditches at the planning stage and also immediately evaluate the efficiency of the  
486 whole system (slope-ditch) for each geometric configuration, material properties and retention  
487 level assumed.

488 • A triangular ditch with constant foreslope steepness is more efficient than a deep flat-bottom  
489 ditch, and the former is more effective for the steepest gradient ( $\alpha_d > 14^\circ$ ). Furthermore, wider  
490 triangular ditches of less depth reduce the risk of vehicle overturning, increasing road safety, and  
491 simplifies ditch maintenance.

492 • The improved ditch design (reduction of catchment area width) proposed in this study compared  
493 to previous studies is associated with the criterion assumed when modelling (random nature of  
494 the launch point height). This assumed hypothesis is adequate for common and frequent  
495 geomechanical conditions, especially regarding volcanic geomaterials, and offers more  
496 economical and optimized solutions during the service life of transport infrastructures. These  
497 rockfall protection areas constitute non-structural defence measures with low environmental  
498 impact and reduced cost in volcanic territories.

499

## 500 **References**

501 [1] Santamaría Arias J, Ballester Muñoz F, Luis Fonseca R, Torres Vilas JA (1996). Protección  
502 contra desprendimientos de rocas, pantallas dinámicas. Centro de Publicaciones del Ministerio  
503 de Fomento. Madrid. ISBN: 84-498-0253-9. D.L.: M-40877-1996 (in Spanish).

504 [2] Ritchie AM (1963). Evaluation of rockfall and its control. Record, 17 Highway Research Board:  
505 13-28.

506 [3] Pierson LA, Gullixson CF, Chassie RG (2001). Rockfall catchment area design guide. Final  
507 Report SPR-3(032). Oregon Department of Transportation Research Group. U.S. Federal  
508 Highway Administration. Report n°: FHWA-OR-RD-02-04.

- 509 [4] Pantelidis L (2010). Rock catchment area design charts. In: GeoFlorida 2010: Advances in  
510 Analysis, Modelling & Design (GSP 199). Department of Civil Infrastructure Engineering,  
511 Technological Educational Institute of Thessaloniki, Greece.
- 512 [5] Gomes GJC, Sobreira FG, Lana MS (2012). Design of highway rock slopes catchment area.  
513 Road materials and pavement design 13, 2:396-402. DOI: [10.1080/14680629.2012.685841](https://doi.org/10.1080/14680629.2012.685841)
- 514 [6] Federal Highway Administration (1989). Rock slopes: design, excavation, stabilization.  
515 Publication FHWA-TS-89-045. McLean, Virginia: Turner-Fairbank Highway Research Center.
- 516 [7] Spang RM, Rautenstrauch RW (1988). Empirical and mathematical approaches to rockfall  
517 protection and their practical application. Rock Mechanics and Rock Engineering, 23:207-209.
- 518 [8] Okura Y, Kitahara H, Sammori T (2000). Fluidization in dry landslides. Engineering Geology,  
519 56:347–360. DOI: [10.1016/S0013-7952\(99\)00118-0](https://doi.org/10.1016/S0013-7952(99)00118-0)
- 520 [9] Giani GP, Giacomini A., Migliazza M, Segalini A (2004). Experimental and theoretical studies  
521 to improve rock fall analysis and protection work design. Rock Mechanics and Rock  
522 Engineering, 37(5):369–389. DOI: [10.1007/s00603-004-0027-2](https://doi.org/10.1007/s00603-004-0027-2)
- 523 [10] Labiouse V, Heidenreich B (2009). Half-scale experimental study of rockfall impacts on sandy  
524 slopes. Natural Hazards and Earth System Science, 9(6):1981-1993. DOI: [10.5194/nhess-9-  
525 1981-2009](https://doi.org/10.5194/nhess-9-1981-2009)
- 526 [11] Ye SQ, Chen HK, Xu J (2011). Rockfalls movement mode and movement features by field tests.  
527 Tumu Jianzhu yu Huanjing Gongcheng/Journal of Civil, Architectural and Environmental  
528 Engineering, 33 (2): 18-23+44. DOI: [10.11835/j.issn.1674-4764.2011.02.005](https://doi.org/10.11835/j.issn.1674-4764.2011.02.005)
- 529 [12] Vijayakumar S, Yacoub T, Curran J (2011). A study of rock shape and slope irregularity on rock  
530 fall impact distance. 45th US Rock Mechanics / Geomechanics Symposium.
- 531 [13] Bourrier F, Berger F, Tardif P, Dorren L, Hungr O (2012). Rockfall rebound: comparison of  
532 detailed field experiments and alternative modelling approaches. Earth Surface Processes and  
533 Landforms, 37:656–665. DOI: [10.1002/esp.3202](https://doi.org/10.1002/esp.3202)
- 534 [14] Duncan C, Wyllie DC (2014). Calibration of rock fall modelling parameters. International  
535 Journal of Rock Mechanics and Mining Sciences, 67:170-180;  
536 <https://doi.org/10.1016/j.ijrmms.2013.10.002>
- 537 [15] Ferrari F, Thoeni K, Giacomini A, Lambert C (2016). A rapid approach to estimate the rockfall  
538 energies and distances at the base of rock cliffs. Georisk: Assessment and Management of Risk  
539 for Engineered Systems and Geohazards, 10(3):179–199. DOI:  
540 [10.1080/17499518.2016.1139729](https://doi.org/10.1080/17499518.2016.1139729)
- 541 [16] Asteriou P, Tsiambaos G (2018). Effect of impact velocity, block mass and hardness on the  
542 coefficients of restitution for rockfall analysis. International Journal of Rock Mechanics and  
543 Mining Sciences, 106:41–50. DOI: [10.1016/j.ijrmms.2018.04.001](https://doi.org/10.1016/j.ijrmms.2018.04.001)
- 544 [17] Pierson LA, Davis SA, Pfeiffer TJ (1994). The Nature of Rockfall as the Basis for a New

- 545 Catchment Area Design Criteria For 0.25H:1V Slopes. Oregon Department of Transportation,  
546 Report No. FHWA-OR-GT-95-05.
- 547 [18] Hoek, E. (1987). Rockfall – A program in Basic for the analysis of rockfalls from slopes.  
548 Vancouver BC: Golder and Associates.
- 549 [19] Wu, S. (1987). Rockfall evaluation by computer simulation. Transportation Research Record,  
550 National Research Board, Washington DC, 1031:1–5.
- 551 [20] Pfeiffer TJ, Higgins JA (1990). Rockfall hazard analysis using the Colorado rockfall simulation  
552 program. Transportation Research Record, No. 1288, National Research Board, Washington DC,  
553 117–126.
- 554 [21] RocScience (2011). Computer program RocFall. Toronto, Canada: RocScienceInc.
- 555 [22] Nishikawa Y, Masuya H, Moriguti Y (2012). Three dimensional simulation of rockfall motion  
556 with consideration of roughness of the slope surface. Transactions of the Japan Society for  
557 Computational Engineering and Science 2012: 3.
- 558 [23] Siddique T, Pradhan SP, Vishal V. (2019). Rockfall: A Specific Case of Landslide. In: Pradhan  
559 S., Vishal V., Singh T. (eds) Landslides: Theory, Practice and Modelling. Advances in Natural  
560 and Technological Hazards Research. Springer, Cham, vol 50:61-81.  
561 [https://doi.org/10.1007/978-3-319-77377-3\\_4](https://doi.org/10.1007/978-3-319-77377-3_4)
- 562 [24] Pantelidis L, Kokkalis A (2011). Designing passive rockfall measures based on computer  
563 simulation and field experience to enhance highway safety. International Journal of Rock  
564 Mechanics and Mining Sciences 48(8):1369-1375. DOI: 10.1016/j.ijrmms.2011.09.008
- 565 [25] Pfeiffer T and Bowen T (1989). Computer simulation of rockfalls. Environmental &  
566 Engineering Geoscience, 26 (1):135-146.
- 567 [26] Andrew R, Hume H, Bartingale R, Rock A, Zhang R (2012). CRSP-3D User's Manual  
568 (Colorado Rockfall Simulation Program). Central Federal Lands Highway Division (FLH) of the  
569 Federal Highway Administration (FHWA). Publication No. FHWA-CFL/TD-12-007.
- 570 [27] Rodriguez-Losada JA, Hernandez-Gutierrez LE, Olalla C, Perucho A, Serrano A, del Potro R  
571 (2007). The volcanic rocks of the Canary Islands. Geotechnical properties. In: Volcanic Rocks  
572 (Eds. Malheiro & Nunes): 53-57. Taylor & Francis Group. London. ISBN 978-0-415-45140-6.
- 573 [28] Rodriguez-Losada JA, Hernandez-Gutierrez LE, Olalla C, Perucho A, Serrano A, Eff-Darwich  
574 A (2009). Geomechanical parameters of intact rocks and rock masses from the Canary Islands:  
575 Implications on their flank stability. Journal of Volcanology And Geothermal Research, 182 (1-  
576 2):67. DOI: 10.1016/j.jvolgeores.2009.01.032
- 577 [29] García-González C, Yepes J, Franesqui MA (2020). Geomechanical characterization of  
578 volcanic aggregates for paving construction applications and correlation with the rock  
579 properties. Transportation Geotechnics, 24:100383.  
580 <https://doi.org/10.1016/j.trgeo.2020.100383>

- 581 [30] Ziaei A, Ahangari K (2018). The effect of topography on stability of shallow tunnels case study:  
582 The diversion and conveyance tunnels of Safa Dam. *Transportation Geotechnics*, 14:126-135.  
583 <https://doi.org/10.1016/j.trgeo.2017.12.001>
- 584 [31] Alejano LR, Pons B, Bastante FG, Alonso E, Stockhausen HW (2007). Slope geometry design  
585 as a means for controlling rockfalls in quarries. *International Journal of Rock Mechanics and*  
586 *Mining Sciences*, 44(6):903–21. DOI: [10.1016/j.ijrmms.2007.02.001](https://doi.org/10.1016/j.ijrmms.2007.02.001)
- 587 [32] Vishal V, Siddique T, Purohit R, Phophliya MK, Pradhan SP (2017). Hazard assessment in  
588 rockfall-prone Himalayan slopes along National Highway-58, India: rating and simulation.  
589 *Natural Hazards*, 85(1):487-503. <https://doi.org/10.1007/s11069-016-2563-y>
- 590 [33] Ye SQ, Shangqing G, Yang ZY, Hui, L (2014). Model test for falling-rock motion  
591 characteristics on composite slope section. *Electronic Journal of Geotechnical Engineering*, 19  
592 U:6161- 6171.
- 593 [34] Asteriou P, Saroglou H, Tsiambaos G (2012). Geotechnical and kinematic parameters affecting  
594 the coefficients of restitution for rockfall analysis. *International Journal of Rock Mechanics and*  
595 *Mining Sciences*, 54:103–113. DOI: [10.1016/j.ijrmms.2012.05.029](https://doi.org/10.1016/j.ijrmms.2012.05.029)  
596

597 **Supplementary material**

598 Supplementary data associated with this article (Table 7 and Fig. 13) can be found in the online version.

599

600 **Table 7.** Statistical parameters of the  $X_{stop}^*$  evaluated: (Ds) Standard Deviation; ( $H_t$ ) Slope height; (K)  
601 Kurtosis Index; (M) Averaged value of  $X_{stop}^*$ ; (Ref) Reference code (see \*1); (S) Skewness.

602 (\*1) [ $H_t$ \_(H:V) $_t$   $W_d$ \_(H:V) $_d$  L\_Fb\_Sb] Code to designate each evaluated arrangement according to its characteristic:  
603 ( $H_t$ ) Slope height in m; (H/V) $_t$  Slope gradient expressed as the relation of horizontal and vertical distance; ( $W_d$ ) Ditch  
604 width in m; (H/V) $_d$  Ditch foreslope expressed as the relation of the horizontal and vertical distance; (L) Lithotype:  
605 HR, Hard Rock; SR, Soft Rock; (F $_b$ ) Block shape (Cu, Cube; Sp, Sphere; Cy, Cylinder); (S $_b$ ) Block size.

606

607 **Fig. 13.** Graphic design charts for different slope-ditch configurations correlating the ditch width with the  
608 percentage of rock retention. Input parameters: ( $H_t$ ) Slope height in m; (H/V) $_t$  Slope gradient expressed as  
609 the relation of the horizontal and vertical distance; Lithotype (HR, Hard Rock; SR, Soft Rock). The solid  
610 line represents a flat ditch (1H/0V), the dashed line a 10° ditch (6H/1V), and the dotted line a 14° ditch  
611 (4H/1V).